International Journal of Applied Pharmaceutics

ISSN- 0975-7058 Vol 16, Issue 5, 2024

Original Article

SMART CHITOSAN-BASED MICROBEAD FORMULATION FOR COLON-TARGETED DELIVERY OF LACTOFERRIN

LUQMAN OLAOYE[1], AZAD SADRADDIN[2], SHWANA BRAIM[1*]

[1]Department of Chemistry and Forensic Science, School of Science and Technology, Nottingham Trent University, Clifton Lane, Nottingham, NG11 8NS, United Kingdom. [2]Department of Chemistry, Salahaddin University-Erbil, Kurdistan Region
[*]Corresponding author: Shwana Braim; [*]Email: shwana.braim@ntu.ac.uk

Received: 21 Apr 2024, Revised and Accepted: 26 Jun 2024

ABSTRACT

Objective: This study aims to develop a novel smart formulation based on dual-responsive Polyethylene Glycol Methacrylate-Grafted-Chitosan (PEGMA-g-Cs) copolymers for the controlled delivery of Lactoferrin. The goal is to enhance the bioavailability and therapeutic efficacy of Lactoferrin in treating colorectal cancer, addressing its rapid degradation in a highly acidic gastric environment.

Methods: Gold-coated Superparamagnetic Iron Oxide Nanoparticles (Au-SPIONs) were synthesized and loaded into PEGMA-g-Cs microspheres. Transmission Electron Microscopy (TEM), Scanning Electron Microscopy (SEM), Proton Nuclear Magnetic Resonance (HNMR), X-Ray Diffraction (XRD), Infrared Spectroscopy (IR), UV-visible spectrophotometry (UV-Vis), optical microscopy, and Dynamic Light Scattering (DLS) were used to characterise the synthesized materials. Drug loading and release studies of lactoferrin-loaded microbead formulations were conducted to evaluate encapsulation efficiency, loading capacity, and release profiles.

Results: The lactoferrin-loaded microbead formulations demonstrated excellent encapsulation efficiency and loading capacity. Specifically, Encapsulation Efficiency (EE) was 77% and Loading Capacity (LC) was 4.99% for the homogenizer batch, while the magnetic stirring batch achieved 86% EE and 3.12% LC. The formulation exhibited minimal release (<20%) in Simulated Gastric Fluid (SGF) and almost complete release in Simulated Colonic Fluid (SCF). The 3-[4,5-Dimethylthiazol-2-Yl]-2,5-Diphenyl Tetrazolium Bromide (MTT) cell cytotoxicity assay in human CaCo-2 colon cancer cells revealed a significant reduction in cell proliferation following treatment with the new formulations.

Conclusion: The findings suggest that the new formulation can be a promising approach for the targeted delivery of Lactoferrin, thereby improving the efficacy of colorectal cancer treatment by enhancing the bioavailability of lactoferrin.

Keywords: Lactoferrin, Colorectal cancer, Chitosan, PEGMA-g-Cs, Smart formulation, Targeted delivery

DOI: https://dx.doi.org/10.22159/ijap.2024v16i5.51185 Journal homepage: https://innovareacademics.in/journals/index.php/ijap

INTRODUCTION

Colorectal cancer is a global health challenge that affects millions of people worldwide and demands innovative therapeutic strategies to improve patient outcomes [1]. There is a growing focus on targeted therapies and the development of new sustainable formulations that can effectively treat colorectal cancer while minimising the side effects of current chemotherapeutic treatments [2, 3]. Recent studies have shown that some forms of Lactoferrin have the potential to treat various diseases and conditions, including infections, cancer, and inflammation [4–13]. However, lactoferrin's therapeutic efficacy is limited by its rapid degradation in a highly acidic gastric environment. Therefore, developing a controlled delivery system for lactoferrin could enhance its bioavailability and improve its therapeutic outcomes. Leveraging lactoferrin's potential, researchers have explored strategies such as lactoferrin-coated lipid nanoparticles and polymer-based micelles to enhance drug solubility, stability, and controlled release, thereby optimising therapeutic efficacy [14, 15]. The integration of lactoferrin into hybrid nano/micro systems magnifies its therapeutic capabilities. By amalgamating lactoferrin with other bioactive compounds or nanomaterials, multifunctional platforms are created. Noteworthy examples include lactoferrin-polymer hybrid nanoparticles, where synergistic interactions enhance therapeutic outcomes [16, 17]. Responsive nanocarriers have elevated the precision of lactoferrin-based formulations. Incorporating stimuli-responsive elements such as temperature-sensitive elastin-like polypeptides or block copolymers permits targeted drug release triggered by specific cues within the tumour microenvironment [18]. Lactoferrin's multifaceted nature extends to photothermal therapy. The integration of lactoferrin-conjugated gold nanoparticles facilitates localised hyperthermia upon laser irradiation, leading to targeted cancer cell ablation [19]. Microfluidics has introduced a paradigm shift in lactoferrin formulation because it can offer meticulous control over particle attributes, ensuring consistent and reproducible lactoferrin-based formulations [20, 21]. This study addresses the development of a novel multi-responsive formulation for the controlled delivery of lactoferrin.

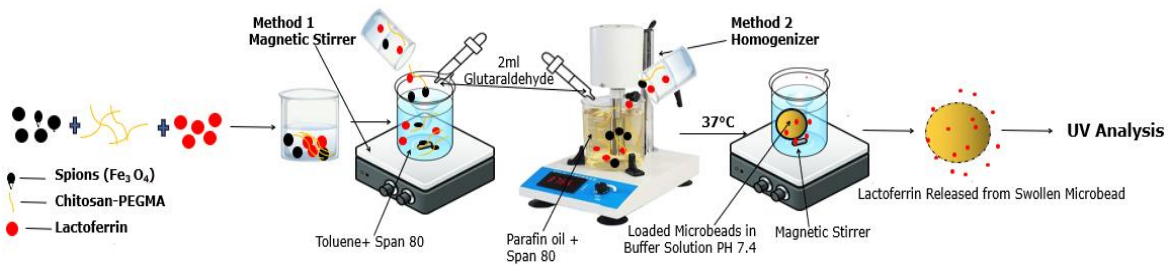

Fig. 1: Schematic illustration of the synthesis process of a dual-responsive PEGMA-g-Cs formulation for colon-targeted delivery of lactoferrin

MATERIALS AND METHODS

Materials

Materials used in this study included low and medium molecular weight chitosan, 35% ammonium solution, glacial acetic acid, NaOH, Glutaraldehyde, Tween 80, Span 80, sodium Tripolyphosphate (TPP), Poly(Ethylene Glycol) Methacrylate (PEGMA), toluene, sodium citrate, and paraffin oil. Each of these chemicals was bought from Sigma Aldrich.

Synthesis of gold-coated superparamagnetic iron oxide nanoparticles (Au-SPIONs)

Superparamagnetic Iron Oxide Nanoparticles (SPIONs) were successfully synthesised through the chemical coprecipitation method, followed by gold coating [22, 23]. 5.40 g of $FeCl_3 \cdot 6H_2O$ and 2 g of $FeCl_2 \cdot 4H_2O$ (2:1 mole ratio) were dissolved in 50 ml of deionized water (solution A) using a magnetic stirrer under nitrogen purging at 40 °C. 12 ml of ammonia solution was added dropwise to solution A, followed by a 20 min wait. Then, 8.8 g of sodium citrate was introduced, and the temperature was increased to 90 °C. The mixture was maintained at 90 °C with continuous nitrogen purging and stirring for 1 h. After cooling to room temperature, a black precipitate formed, which was thoroughly washed with water and ethanol. The resultant sample was separated using a permanent magnet and dried in a vacuum oven at 35 °C for 5 h. Gold coating was conducted by stirring the prepared magnetic particle solution in a gold chloride and sodium citrate solution.

Synthesis of polyethylene glycol methacrylate-grafted-chitosan (PEGMA-g-Cs)

PEGMA-g-Cs copolymers were synthesised by the Michael addition reaction [24]. A 1% (w/w) low molecular weight chitosan solution was prepared by dissolving chitosan in acetic acid (AA). 50 ml of this solution was placed into a 250 ml two-neck round-bottom flask equipped with a reflux condenser. The solution was heated to 45 °C with continuous nitrogen purging and vigorous stirring for 35 min. 5 ml of PEGMA was added dropwise, maintaining a 2:1 molar ratio of NH2 groups in chitosan to PEGMA. The temperature was then raised to 55 °C and maintained for 48 h. The resulting light brown copolymer solution was washed twice with dry acetone and twice with methanol, each followed by centrifugation at 4700 rpm for 10 min at 5 °C. The purified copolymer was dried at 25 °C for 24 h and characterised using Fourier-Transform Infrared Spectroscopy (FT-IR).

Synthesis of smart microbeads using magnetic stirrer

The emulsification internal gelation method was used to prepare smart microbeads. 100 ml of toluene was mixed with 2 ml of Span 80 and stirred for 10 min to form Solution A. A 1% (w/w) solution of 50 ml of low molecular weight chitosan in acetic acid was prepared, to which 1 ml of Tween 80 and 50 µl of magnetic nanoparticles were added. This solution (Solution B) was sonicated for 10 min before being added dropwise to Solution A under vigorous stirring. Solution C was formed and stirred for 1 h to encapsulate the magnetic nanoparticles within the chitosan beads. Then, a 5% TPP solution was added to Solution C to facilitate cross-linking. The chitosan-magnetic nanoparticle beads were rinsed with acetone and dried at 25 °C for 24 h.

Synthesis of magnetic microbeads using homogenizer

100 ml of paraffin oil was mixed with 3 ml of Span 80 and stirred vigorously for 15 min to create Solution A. A 1% (w/w) solution of 50 ml low molecular weight chitosan in acetic acid was prepared, with 1.5 ml of Tween 80 and 50 ml of nanoparticles added. This mixture was sonicated for 10 min to form Solution B. Solution B was added dropwise to Solution A with continuous stirring. Solution C was stirred for 50 min, followed by the addition of 2 ml of glutaraldehyde for cross-linking. The chitosan-nanoparticle beads were rinsed with acetone and dried at 25 °C for 24 h.

Synthesis of lactoferrin-loaded formulation using magnetic stirrer (F1)

25 mg of lactoferrin was dissolved in 2.5 ml of water to form Solution A. Solution A was mixed with 10 g of 1% PEGMA-g-Cs in 1% acetic acid to create Solution B. 200 µl of SPIONs was added to Solution B, forming Solution C. Solution C was added to 100 ml of toluene containing 2 ml of Span 80 (Solution D) while stirring at 850 rpm, resulting in Solution E. A total of 2 h were required for the reaction after adding 1 ml of glutaraldehyde and another 1 ml after 50 min. The lactoferrin-loaded microbeads were washed with petroleum ether and dried at 25 °C for 12 h. A comprehensive analysis was performed using UV spectrophotometry.

Synthesis of lactoferrin-loaded formulation using homogenizer (F2)

25 mg of lactoferrin was dissolved in 2.5 ml of water to form Solution A. Then, this solution was mixed with 10 g of 1% PEGMA-g-Cs in 1% acetic acid to create Solution B. 200 µl of SPIONs was added to the second solution, forming Solution C. the last solution was added to 100 ml of paraffin oil containing 2 ml of Span 80 while stirring at 700 rpm,. After 10 min, 1 ml of glutaraldehyde was added, followed by another 1 ml after 50 min, with a total reaction time of 2 h. The drug-loaded microbeads were washed with petroleum ether and dried at 25 °C for 12 h. SEM and UV-Vis spectrophotometry were used to characterise synthesised materials.

Transmission Electron Microscopy (TEM)

Samples for TEM (model: JEM-2100 Plus, maker: JOEL) were prepared using the drop-casting method on a copper TEM grid with a carbon support film. A 10 µl sample solution was applied to the grid and allowed to rest for 15 min. The excess solution was removed, and the grid was placed in the TEM for imaging.

Scanning Electron Microscopy (SEM)

SEM (model: JSM-7100f, maker: JOEL) was used to visualise the morphology, size, and shape of nanoparticles and microbeads. Samples were prepared by sprinkling them onto double-sided carbon tape attached to an aluminium stub. This setup was mounted on the sample holder for SEM analysis. Slow scan mode and stage control adjustments were used for detailed imaging.

FIT-IR spectroscopy

FT-IR spectra were acquired using a PerkinElmer Spectrum (Version 10.03.07) with a lithium tantalate mid-infrared detector. The instrument was cleaned with methanol, and a background spectrum was obtained before sample analysis. The prepared sample was placed on the sample stage of the FT-IR spectrometer. Spectra were collected over a wavelength range of 4000 to 400 cm^{-1}. The recorded spectra were automatically corrected for background noise using the instrument's software. To ensure reproducibility, each sample was analysed in triplicate, and the spectra were compared for consistency.

Encapsulation efficiency and *in vitro* release studies

The concentration of Lactoferrin was evaluated using the UV-Vis spectrophotometry method (UV5Bio Spectrophotometer) at a wavelength of 280 nm. A range of Lactoferrin standard solutions were prepared to create a linear calibration curve with an R^2 value of 0.9996. The calibration curve was used to determine the unknown concentration of Lactoferrin (loaded or released) in the formulation. Triplicate measurements were performed. To study the *in vitro* release of encapsulated Lactoferrin, Simulated Gastric Fluid (SGF pH 1.2), Simulated Intestinal Fluid (SIF pH 6.5), and Simulated Colonic Fluid (SCF pH 7.4) conditions without enzymes were employed. First, the formulation was stirred in SGF at 100 rpm for 2 h. Next, immersed in a SCF for 22 h. Samples were collected at various time intervals for spectrophotometric measurement of Lactoferrin concentration. Then, the encapsulation efficiency (EE%), drug loading capacity (LC%), and drug release (R%) were calculated using equations 1, 2, and 3, respectively.

$$\text{EE\%} = \left(\frac{\text{weight of drug encapsulated}}{\text{weight of drug used}}\right) * 100 \quad \ldots\ldots (1)$$

$$LC\% = \left(\frac{\text{weight of drug encapsulated}}{\text{weight of drug formulation}}\right) * 100 \ \ldots\ldots (2)$$

$$R\% = \left(\frac{\text{weight of drug released after this time}}{\text{weight of drug formulation}}\right) * 100 \ \ldots\ldots (3)$$

Finally, the cumulative release of Lactoferrin were plotted against the time period.

Cell culture and *in vitro* cytotoxicity study

Caco-2 cells, as a model of huma colorectal cancer cells, were cultured in Dulbecco's Modified Eagle Medium (DMEM) medium with 10% Fetal Bovine Serum (FBS), 1% of L-glutamine, 50 µg/ml streptomycin, and 50 IU/ml penicillin in a CO2 and 37 °C incubator. The *in vitro* cytotoxicity of free Lactoferrin and prepared formulations on Caco-2 cells was assessed by 3-(4,5-Dimethylthiazol-2-Yl)-2,5-Diphenyl Tetrazolium Bromide (MTT) assay over 48 h. First, Caco-2 cells were seeded (5000 cells/well) in a 96-well plate containing 100 µl of cell culture medium and left overnight to adhere. Next, the DMEM was replaced by fresh medium containing different concentrations of Lactoferrin or a prepared formulation and incubated for 24 h. Then, the medium was aspirated and 100 µl of MTT solution in DMEM was added, followed by incubation for an additional 4 h in a CO_2 and 37 °C incubator. Finally, the MTT solution and the absorbance were recorded using a microplate reader (Bio-Rad, USA) at 570 nm, background wavelength of 690 nm. Experiments were repeated in triplicate or more, and Microsoft Excel was used to do statistical analysis.

RESULTS AND DISCUSSION

Synthesis and characterization of Au-SPIONs

Gold-coated magnetic nanoparticles were synthesised by chemical coprecipitation followed by gold coating. TEM and SEM characterizations were conducted to evaluate the size, shape, composition, and surface morphologies of the prepared nanoparticles. Fig. 1 shows SEM and TEM images. The results show that Au-SPIONs have a regular shape and an average size of less than 10 nm. These unique properties hold great promise for drug delivery applications [25, 26].

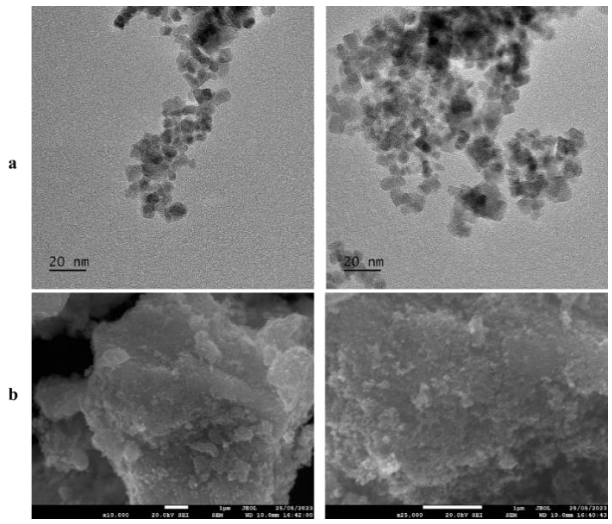

Fig. 2: (a) TEM and (b) SEM images/micrographs of gold-coated SPIONs

Synthesis and characterizations of PEGMA-g-Cs and lactoferrin-loaded formulations

PEGMA was grafted on chitosan to improve swelling behaviour and add thermo-responsive properties. Fourier transform infrared (FT-IR) and HNMR spectroscopy techniques were used to investigate the structural properties of synthesised copolymers. FT-IR spectra of free polymers (chitosan and PEGMA) and PEGMA-g-Chitosan copolymers. The distinct peaks associated with the ether bond (-C-O-C-) in PEGMA and the amide bond (-NH2) in chitosan provide evidence of successful copolymerization, as shown in fig. 3 below. When these peaks show up or go away in the FT-IR spectrum, it means that the reaction is over and the copolymer has been formed. The presence of a new distinctive peak in the 1100–1300 cm^{-1} range for PEGMA-g-Chitosan is strong evidence of successful grafting of PEGMA on Chitosan. This peak is caused by the-C-O-C-in the PEGMA and shows that the PEGMA parts are fully incorporated into the copolymer structure. The appearance of this peak proves that the chemical changes of the separate parts have led to the formation of a cohesive copolymer [27]. Another significant change observed through FT-IR is the shift in peaks related to amide bond formation. The peak corresponding to the amide I band (-C=O) around 1650 cm^{-1}, indicative of carbonyl stretching, shifts to a higher frequency. This shift aligns with the establishment of amide bonds between chitosan and PEGMA, underscoring their interaction. Similarly, the peak around 1590 cm^{-1}, representing the amide II band (-NH bending and-C-N stretching), also shifts to a higher frequency. These shifts substantiate the covalent bonding between chitosan and PEGMA, affirming successful copolymerization. An intriguing aspect of the FT-IR data analysis pertains to the identification of the C=C double bond of PEGMA in the chitosan-PEGMA copolymer. The peak centred around 1635–1640 cm^{-1} signifies the presence of this double bond and corresponds to Michael's addition reaction. This addition reaction at the C=C double bond of the PEGMA monomer evidences the successful incorporation of PEGMA into the copolymer structure [26].

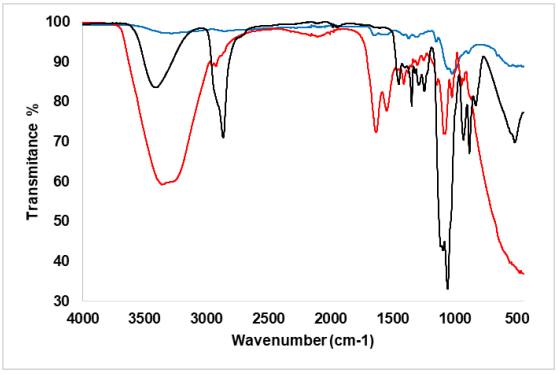

Fig. 3: FT-IR spectra of chitosan (-blue line), PEGMA-g-Cs copolymer (-red line) and only PEGMA (-black line) confirming successful preparation of PEGMA-g-Cs

[1]HNMR (JOEL ECZS series, 400 MHz) was also used to obtain more detailed information about the chemical structure of the newly devel ped polymer. Fig. 4 shows the [1]H-NMR spectra of the PEGMA-g-Chitosan copolymer. The diagnostic peaks are as follows: 1.76 ppm (3H, s, CH3 of Chitosan). 2.93 ppm (1H, s, H-2 of Chitosan), 3.21 ppm (3H, s, methyl group of PEGMA), peaks observed in the range of 3.51–3.59 ppm (m, H-3, H-4, H-5, H-6, H-6' of chitosan and –OCH2–(c),-CH2 (b) of PEG), 4.17 ppm (2H, s,-OCH2-of PEG chain). The combination of IR and [1]HNMR data indicates that the PEGMA-g-Chitosan copolymer was successfully synthesised.

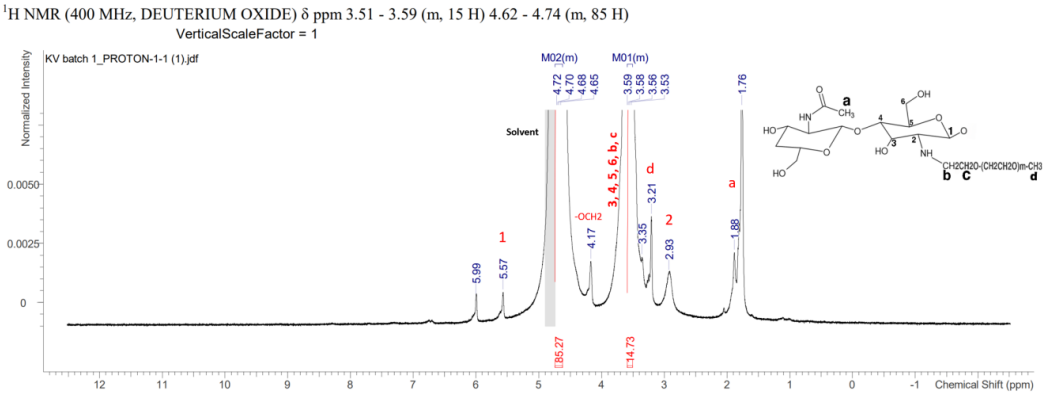

Fig. 4: HNMR spectrum of PEGMA-g-Cs copolymer dissolved in D_2O

Because particle size influences drug accumulation in the inflammatory colon, it is crucial to consider particle size, morphology, and size distribution when developing colon-specific drug delivery techniques. The size and morphology of the microbead were investigated by optical microscopy and SEM. Fig. 5a shows optical microscopy images of PEGMA-g-Cs microbeads, It is clear that synthesised microspheres have smooth spherical shape, are almost monodisperse, and their average size is around 1 µm. This indicates the potential significance of prepared microbeads for oral drug delivery applications and facilitating efficient drug loading and controlled release [28]. Fig. 5b shows the homogeneous distribution of magnetic nanoparticles within microbeads. SEM photographs are presented in fig. 5c (low magnification) and 5d (high magnification), which further confirms that monodisperse and spherical-shaped microbead formulations were prepared.

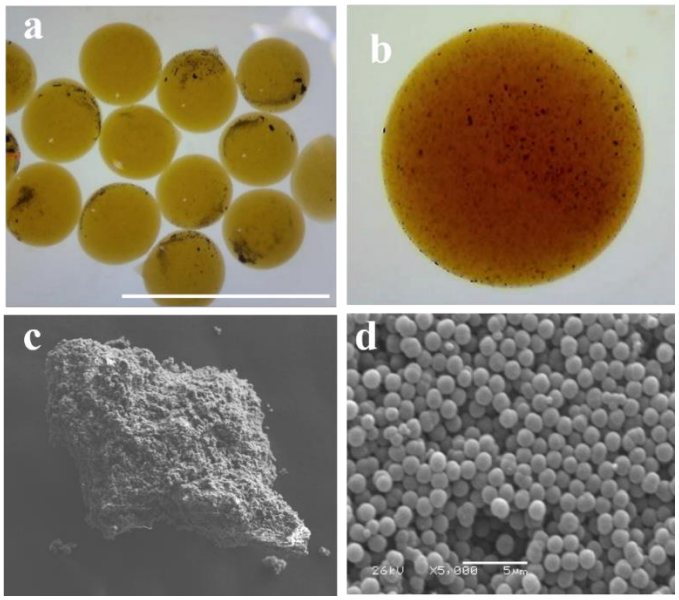

Fig. 5: Optical microscopy and SEM images of PEGMA-g-Cs microbeads. The magnifications for optical images (a) and (b) are 10x and 40x, respectively. Whereas the magnifications for SEM images (c) and (d) are 1000 and 5000, respectively

Finally, the swelling behaviour of microbeads in solutions with different pH values was evaluated. This is an important factor in the encapsulation, retention, and controlled release of Lactoferrin. The result revealed a significant difference in swelling between SGF (pH 1.2) and SIF (pH 7.4). The swelling in SGF was almost negligible, however, the swelling in SIF was about 290%.

Drug loading and release profile

UV-Vis spectrophotometry and the calibration curve have been used to look at the Lactoferrin loading capacity, encapsulation efficiency, and release dynamics. Also, simulated gastrointestinal conditions without enzymes were used to mimic human gastrointestinal tract physiological conditions. The results revealed that EE was 77% and LC was 4.99% for the homogenizer batch, while EE was 86% and LC was 3.1155% for the magnetic stirring batch.

Drug release studies were conducted at pH values of 1.2, 6.5, and 7.4, which are similar to the pH values of the stomach, small intestine, and colon, respectively. The pH-dependent Lactoferrin release from PEGMA-g-Cs demonstrated a remarkable reliance on the buffer system's pH. The

formulation exhibited minimal release (<20%) and retained most of the Lactoferrin in the SGF, however, almost all the remaining Lactoferrin was released in the SIF. Fig. 6 shows the release profile of the Lactoferrin-loaded formulations. No significant difference can be seen between samples prepared via stirring and homogenization methods.

The drug release profiles underscore the formulation's potential for controlled release and targeted drug delivery. The distinct release kinetics exhibited by the two batches highlight the role of formulation techniques in modulating release behaviour. The high encapsulation efficiency and varying release profiles pave the way for tailored drug delivery strategies.

As research continues, refining formulation methods and investigating underlying mechanisms are imperative for optimising drug release profiles and enhancing therapeutic efficacy.

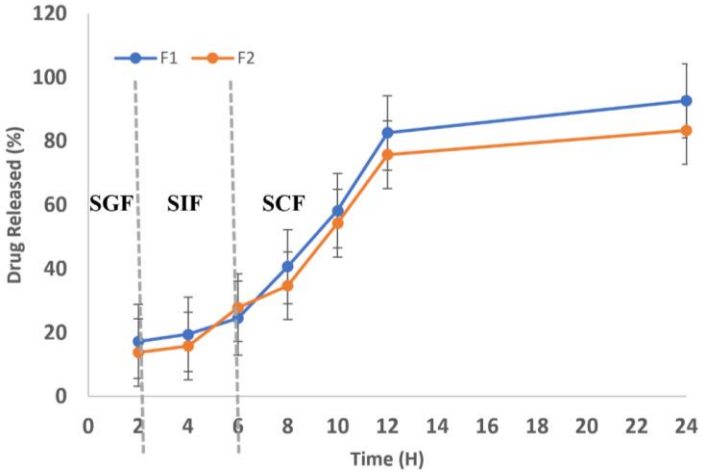

Fig. 6: *In vitro* drug release profiles of lactoferrin-loaded PEGMA-g-Cs formulation. Data were presented as the mean±SD of three independent replications (n=3)

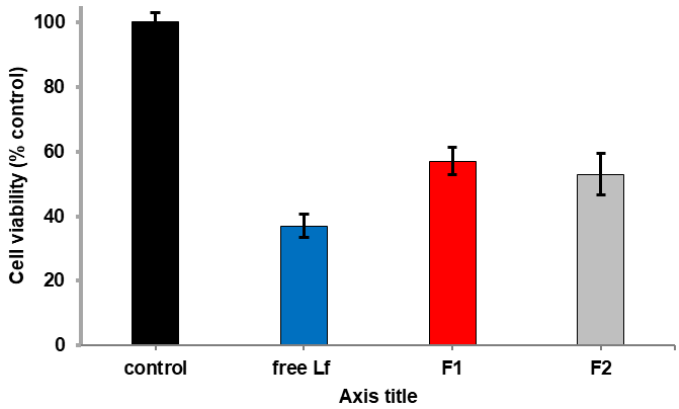

Fig. 7: Cell viability (MTT assays) for free Lactoferrin, F1 and F2 formulations. Data were presented as mean±SD of three independent replications (n=3)

In vitro cell toxicity test

MTT assays were conducted on the Caco-2 human colorectal adenocarcinoma cells to investigate the therapeutic efficacy of the developed formulation. Fig. 7 shows *in vitro* cell toxicity assay results for free Lactoferrin and Lactoferrin-loaded formulations. The results indicate a reduction in cell viability after incubating Caco-2 cells with the developed formulations. The data were presented as the mean±SD of three independent replications.

CONCLUSION

A new smart formulation based on PEGMA-g-Cs was developed for colon-targeted delivery of Lactoferrin, aiming to preserve its bioactivity in the GI tract and enhance its therapeutic efficacy. First, Au-SPION and PEGMA-g-Cs copolymers were prepared. Next, nanoparticles were loaded onto the dual responsive PEGMA-g-Cs microspheres. The synthesised materials were then characterized using TEM, SEM, HNMR, XRD, IR, DLS, UV-Visible spectrophotometry, and optical microscopy. The drug loading and release studies of the lactoferrin-loaded microbead formulation revealed excellent encapsulation efficiency, loading capacity, and release profile. The drug release profiles in the GI tract demonstrated minimal Lactoferrin release in acidic pH conditions, followed by sustained release at a colonic pH. These findings suggest that the new formulation can be a promising approach for the controlled delivery of Lactoferrin, thereby improving the efficacy of colorectal cancer treatment. The MTT cell cytotoxicity assay in human CaCo-2 colon cancer cells showed a reduction in cell proliferation after treatment with the new formulations. The ability to specifically target cancer cells while minimizing damage to healthy tissues is a crucial advancement in the field of cancer treatment.

FUNDING

No funding was received to conduct this study.

AUTHORS CONTRIBUTIONS

Luqman Olaoye conducted the experiments and collected the data. Azad Sadraddin prepared polymers, analysed the data, and wrote the

manuscript. Shwana Braim conceived the study and designed the experiments. All authors reviewed and approved the final manuscript.

CONFLICT OF INTERESTS

The authors declare no competing interests.

REFERENCES

1. Alaryani FS, Turki Alrdahe SS. A review of treatment, risk factors, and incidence of colorectal cancer. Int J App Pharm. 2022;14(1):1-6. doi: 10.22159/ijap.2022v14i1.42820.
2. Muhammed RA, Mohammed S, Visht S, Yassen AO. A review on development of colon targeted drug delivery system. Int J App Pharm. 2024;16(2):12-27. doi: 10.22159/ijap.2024v16i2.49293.
3. Dhas SK, Deshmukh G. Formulation and evaluation of meloxicam microspheres for colon targeted drug delivery. Asian J Pharm Clin Res. 2021;14(8):45-51. doi: 10.22159/ajpcr.2021.v14i8.38482.
4. Patil AS, Puri R, Wakure BS. A review on lactoferrin principle constituent of bovine colostrum: in COVID19. Int J Curr Pharm Sci. 2022;14(3):1-8. doi: 10.22159/ijcpr.2022v14i3.1984.
5. Khan AR, Sadiq IZ, Abdullahi LI, Danlami D, Taneja P. Chemoprotective role of bovine lactoferricin against 7,12 dimethylbenz[a]anthracene induced skin cancer in female swiss albino mice. Int J Pharm Pharm Sci. 2016;8(8):215-22.
6. Mohd KS, Hassan MA, Azemin WA, Dharmaraj S. A review of potential anticancers from antimicrobial peptides. Int J Pharm Pharm Sci. 2015;7:19-26.
7. Coccolini C, Berselli E, Blanco Llamero C, Fathi F, Oliveira MB, Krambeck K. Biomedical and nutritional applications of lactoferrin. Int J Pept Res Ther. 2023;29(5):71. doi: 10.1007/s10989-023-10541-2.
8. Shini VS, Udayarajan CT, Nisha P. A comprehensive review on lactoferrin: a natural multifunctional glycoprotein. Food Funct. 2022;13(23):11954-72. doi: 10.1039/d2fo02371g, PMID 36383056.
9. Cutone A, Ianiro G, Lepanto MS, Rosa L, Valenti P, Bonaccorsi di Patti MC. Lactoferrin in the prevention and treatment of intestinal inflammatory pathologies associated with colorectal cancer development. Cancers. 2020;12(12):3806. doi: 10.3390/cancers12123806, PMID 33348646.
10. Pan S, Weng H, Hu G, Wang S, Zhao T, Yao X. Lactoferrin may inhibit the development of cancer via its immunostimulatory and immunomodulatory activities (review). Int J Oncol. 2021;59(5):85. doi: 10.3892/ijo.2021.5265, PMID 34533200.
11. Kruzel ML, Zimecki M, Actor JK. Lactoferrin in a context of inflammation-induced pathology. Front Immunol. 2017;8:1438. doi: 10.3389/fimmu.2017.01438, PMID 29163511.
12. Abd El-Hack ME, Abdelnour SA, Kamal M, Khafaga AF, Shakoori AM, Bagadood RM. Lactoferrin: antimicrobial impacts, genomic guardian, therapeutic uses and clinical significance for humans and animals. Biomed Pharmacother. 2023;164:114967. doi: 10.1016/j.biopha.2023.114967, PMID 37290189.
13. Kowalczyk P, Kaczynska K, Kleczkowska P, Bukowska Osko I, Kramkowski K, Sulejczak D. The lactoferrin phenomenon-a miracle molecule. Molecules. 2022;27(9):2941. doi: 10.3390/molecules27092941, PMID 35566292.
14. Kuperkar K, Patel D, Atanase LI, Bahadur P. Amphiphilic block copolymers: their structures, and self-assembly to polymeric micelles and polymersomes as drug delivery vehicles. Polymers. 2022;14(21):4702. doi: 10.3390/polym14214702, PMID 36365696.
15. Agwa MM, Sabra S. Lactoferrin coated or conjugated nanomaterials as an active targeting approach in nanomedicine. Int J Biol Macromol. 2021;167:1527-43. doi: 10.1016/j.ijbiomac.2020.11.107, PMID 33212102.
16. Liyanage PY, Hettiarachchi SD, Zhou Y, Ouhtit A, Seven ES, Oztan CY. Nanoparticle-mediated targeted drug delivery for breast cancer treatment. Biochim Biophys Acta Rev Cancer. 2019;1871(2):419-33. doi: 10.1016/j.bbcan.2019.04.006, PMID 31034927.
17. Massodi I, Thomas E, Raucher D. Application of thermally responsive elastin-like polypeptide fused to a lactoferrin-derived peptide for treatment of pancreatic cancer. Molecules. 2009;14(6):1999-2015. doi: 10.3390/molecules14061999, PMID 19513001.
18. Hafez DA, Elkhodairy KA, Teleb M, Elzoghby AO. Nanomedicine-based approaches for improved delivery of phyto-therapeutics for cancer therapy. Expert Opin Drug Deliv. 2020;17(3):279-85. doi: 10.1080/17425247.2020.1723542, PMID 31997666.
19. Shanko ES, van de Burgt Y, Anderson PD, den Toonder JM. Microfluidic magnetic mixing at low reynolds numbers and in stagnant fluids. Micromachines. 2019;10(11):731. doi: 10.3390/mi10110731, PMID 31671753.
20. Jaradat E, Weaver E, Meziane A, Lamprou DA. Microfluidics technology for the design and formulation of nanomedicines. Nanomaterials (Basel). 2021;11(12):3440. doi: 10.3390/nano11123440, PMID 34947789.
21. Kumar S, Anselmo AC, Banerjee A, Zakrewsky M, Mitragotri S. Shape and size-dependent immune response to antigen-carrying nanoparticles. J Control Release. 2015;220(A):141-8. doi: 10.1016/j.jconrel.2015.09.069, PMID 26437263.
22. Tintore M, Mazzini S, Polito L, Marelli M, Latorre A, Somoza A. Gold-coated superparamagnetic nanoparticles for single methyl discrimination in DNA aptamers. Int J Mol Sci. 2015;16(11):27625-39. doi: 10.3390/ijms161126046, PMID 26593913.
23. Stein R, Friedrich B, Mühlberger M, Cebulla N, Schreiber E, Tietze R. Synthesis and characterization of citrate-stabilized gold-coated superparamagnetic iron oxide nanoparticles for biomedical applications. Molecules. 2020;25(19):4425. doi: 10.3390/molecules25194425, PMID 32993144.
24. Logigan CL, Delaite C, Tiron CE, Peptu C, Popa M, Peptu CA. Chitosan grafted poly (Ethylene Glycol) methyl ether acrylate particulate hydrogels for drug delivery applications. Gels. 2022;8(8):494. doi: 10.3390/gels8080494, PMID 36005095.
25. Mosafer J, Teymouri M. Comparative study of superparamagnetic iron oxide/doxorubicin co-loaded poly (lactic-co-glycolic acid) nanospheres prepared by different emulsion solvent evaporation methods. Artif Cells Nanomed Biotechnol. 2018;46(6):1146-55. doi: 10.1080/21691401.2017.1362415, PMID 28789586.
26. Gola A, Kozłowska M, Musiał W. Influence of the poly(ethylene glycol) methyl ether methacrylates on the selected physicochemical properties of thermally sensitive polymeric particles for controlled drug delivery. Polymers. 2022;14(21):4729. doi: 10.3390/polym14214729, PMID 36365721.
27. Braim S, Spiewak K, Brindell M, Heeg D, Alexander C, Monaghan T. Lactoferrin-loaded alginate microparticles to target clostridioides difficile infection. J Pharm Sci. 2019;108(7):2438-46. doi: 10.1016/j.xphs.2019.02.025, PMID 30851342.
28. Mitra A, Dey B. Chitosan microspheres in novel drug delivery systems. Indian J Pharm Sci. 2011;73(4):355-66. doi: 10.4103/0250-474X.95607, PMID 22707817.